Metallic bonding and cluster structure

José M. Soler
Department of Physics, Lyman Laboratory, Harvard University, Cambridge, Massachusetts 02138
and Departamento de Física de la Materia Condensada, Universidad Autónoma de Madrid, E-28049 Madrid, Spain

Marcela R. Beltrán
Instituto de Investigaciones en Materiales, Universidad Nacional Autónoma de México, Apartado Postal 70-360, México Distrito Federal, 01000 Mexico

Karo Michaelian
Instituto de Física, Universidad Nacional Autónoma de México, Apartado Postal 20-364, México Distrito Federal, 01000 Mexico

Ignacio L. Garzón
Departamento de Física de la Materia Condensada, Universidad Autónoma de Madrid, E-28049 Madrid, Spain
and Instituto de Física, Universidad Nacional Autónoma de México, Apartado Postal 20-364, México Distrito Federal, 01000 Mexico

Pablo Ordejón
Institut de Ciéncia de Materials de Barcelona-CSIC, Campus de la U.A.B., 08193 Bellaterra, Barcelona, Spain

Daniel Sánchez-Portal
Department of Physics and Materials Research Laboratory, University of Illinois, Urbana, Illinois 61801
and Departamento de Física de la Materia Condensada, Universidad Autónoma de Madrid, E-28049 Madrid, Spain

Emilio Artacho
Departamento de Física de la Materia Condensada, Universidad Autónoma de Madrid, E-28049 Madrid, Spain
(Received 25 August 1999)

Knowledge of the structure of clusters is essential to predict many of their physical and chemical properties. Using a many-body semiempirical Gupta potential (to perform global minimizations), and first-principles density functional calculations (to confirm the energy ordering of the local minima), we have recently found [Phys. Rev. Lett. **81**, 1600 (1998)] that there are many intermediate-size disordered gold nanoclusters with energy near or below the lowest-energy ordered structure. This is especially surprising because we studied ''magic'' cluster sizes, for which very compact-ordered structures exist. Here, we show how the analysis of the local stress can be used to understand the physical origin of this amorphization. We find that the compact ordered structures, which are very stable for pair potentials, are destabilized by the tendency of metallic bonds to contract at the surface, because of the decreased coordination. The amorphization is also favored by the relatively low energy associated to bondlength and coordination disorder in metals. Although these are very general properties of metallic bonding, we find that they are especially important in the case of gold, and we predict some general trends in the tendency of metallic clusters towards amorphous structures.

I. INTRODUCTION

The lowest energy configuration (global minimum) and the structures of low-energy isomers (local minima) are fundamental properties of clusters because they largely determine their physical and chemical behavior. The case of gold is especially relevant since new molecular nanocrystalline materials, considered as prototypes for electronic nanodevices and biosensors, have recently been synthesized using gold nanoclusters as building blocks.[1–5] Such advances in cluster growth and materials synthesis have motivated a number of theoretical and experimental studies on structural, dynamical, electronic, optical, and other physical and chemical properties of isolated and passivated gold clusters, as well as on the size dependence of these.[6–9] Structural characterization using x-ray powder diffraction (XRPD), high-resolution transmission electron microscopy (HRTEM), and scanning tunneling microscopy (STM) have been performed on passivated Au_N nanoclusters with diameters of 1–2 nm, corresponding to aggregates with $N \sim 40$–200 atoms.[8,9]. On the theoretical side, studies on Au_N clusters in this size range have been done using methods going from molecular-dynamics simulations based on semiempirical *n*-body potentials[6,10–12] to first-principles calculations using density-functional theory (DFT).[13,14]

Despite the existence of sophisticated experimental and theoretical tools to study gold nanoclusters, several problems on their structural properties (most stable cluster configuration, lowest-lying isomers, thermal stability) remain unsolved. The current approach determines the cluster structure from the comparison between experimental images (HRTEM,STM) or structure factors (XRPD) with those calcu-

lated from geometrical models of clusters. Following this approach, a truncated decahedral motif was assigned to the most stable geometry of Au nanoclusters in the size range of 1–2 nm.[8] In another study, several possible geometries have been used to calculate the theoretical HRTEM images of gold nanoclusters.[15] Such images constitute a catalog to be used in a systematic comparison with the experimental results.[15] In principle, the mentioned procedure should be sufficient to determine the cluster structures since those methods have been successfully used for larger metal particles or bulk systems. However, in the case of Au_N clusters with sizes of 1–2 nm, the experimental resolution is not good enough to decompose the broad features in the XRPD structure factors and to obtain a conclusive determination of the structures.[8,9] Several theoretical calculations on the configurations of gold nanoclusters have been made using fixed cluster symmetries as constraints during a local optimization of the structure.[7,8,13] Nevertheless, a global, unconstrained optimization of the cluster structure is necessary for an exhaustive search of minima on the potential energy surface.[11] Additional efforts are thus necessary to elucidate the structural properties of gold nanoclusters and their interplay with other physical properties (electronic, optical, etc.), fundamental to the design of gold-based nanostructured materials.

In recent works,[16–18] we have presented results on the most stable (lowest energy) configurations of intermediate-size (1–1.5 nm) Au_N ($N=38,55,75$) nanoclusters obtained through dynamical and evolutive[19] (genetic/symbiotic) optimization methods using a Gupta *n*-body potential.[20] For the three sizes investigated, corresponding to the so-called magic number clusters,[21] we did not find a single-ordered structure, with a definite symmetry as the global minimum.[16,17] Instead, we obtained a set of many isomers nearly degenerate in energy. Moreover, most of these cluster configurations, including the lowest one, have little or no spatial symmetry, and a pair distribution function typical of glasses. Therefore, they can be classified as amorphouslike. First-principles calculations, using DFT in the local-density approximation (LDA), confirmed the energy ordering of the disordered and ordered isomers.[16]

The existence of amorphous metallic clusters has been predicted before. Sodium clusters, which present electronic magic numbers up to $N\sim1000$, and structural magic numbers for larger sizes, are suspected to be liquid or amorphous up to that size.[22] Doye and Wales have obtained amorphous structures for many cluster sizes using pair potentials,[23] finding that the amorphous state is favored by long potential ranges. They warn, however, that many-body effects might modify these trends,[12] and we will see that this is indeed the case. A disordered structure has also been predicted for the lowest energy configuration of Pt_{13} using DFT-LDA.[24] Regarding gold clusters, Ercolessi *et al.*[10] found that their melting temperature became zero for sizes under ~90 atoms, which suggests that they would be amorphous below this size.

Compared to previous works, our results are surprising in two aspects: the amorphous structures appear to be the global minima even at *magic* cluster sizes, for which very compact ordered structures exist; and the amorphous structures are favored for gold, which has a *shorter* potential range[16,17] than other metals, for which the ordered structures are lower in energy. It must be realized, however, that the energy differences between the amorphous and ordered structures are very small. So small that they are in fact well below the absolute-energy precision of even state-of-the-art first-principles methods. Therefore, one must rely on substantial error cancelations, and it is important to check that the observed trends hold when the precision of the calculations increases, and when different methods are employed. Furthermore, it is essential to analyze the characteristic features of the stable amorphous structures, in order to understand the physical origin of the observed trends and, if possible, use this understanding to predict its effects on different systems. These are the objectives of the present paper.

II. FIRST-PRINCIPLES CALCULATIONS

First of all, we have performed further convergence checks of the first-principles DFT calculations presented in Ref. 16, which confirm the observed trends and even increase the relative stability of the amorphous structures. We have used the SIESTA code,[25,26] which performs a fully self-consistent density-functional (DFT) calculation to solve the standard Kohn-Sham equations[27] in the local or gradient-corrected (spin) density approximations. We use standard norm conserving pseudopotentials[28] in their fully nonlocal form.[29] Flexible linear combinations of numerical (pseudo) atomic orbitals are used as the basis set, allowing for multiple-ζ and polarization orbitals. In order to limit the range of the basis pseudoatomic orbitals (PAO), they are slightly excited by a common ''energy shift'' δE_{PAO}, and truncated at the resulting radial node.[26,30] The basis functions and the electron density are projected onto a uniform real-space grid in order to calculate the Hartree and exchange-correlation potentials and matrix elements. The grid fineness is controlled by the ''energy cutoff'' E_{cut} of the plane waves that can be represented in it without alliasing.[31] Tables I and II show various convergence tests for Au_2 and bulk gold, and for the relative energies of amorphous and ordered cluster structures. In all the cases displayed in Table II, an unconstrained conjugate-gradient structural relaxation using the DFT forces was performed for the ordered and disordered cluster structures. It may be seen that the trends observed with the LDA and a minimal basis set remain unchanged when using a more accurate functional and basis set, and that the amorphous structures are indeed more stable than the ordered ones for all the three sizes studied.

One possibility is that the amorphization is driven by Jahn-Teller deformations due to partially filled electronic shells of the cluster. For example, the simplest electron shell model[32] would predict a partially filled *p* shell for Au_{38}, if only the *s* valence electrons are taken into account. In fact, we do observe such Jahn-Teller effects, and they are included in the energies of the ordered structures in Table II. However, they only amount to displacements of ~0.02 Å and energies of ~0.1 eV for Au_{38}, and therefore they cannot explain the much larger differences of geometry and energy between the disordered and ordered structures.

III. METALLIC POTENTIAL

In order to understand the origin of the relative energies obtained with first-principles electronic structure methods,

TABLE I. Convergence tests, for Au_2 and bulk gold, of our first-principles density-functional method. The first line is our reference calculation, and each of the remaining lines corresponds to changing one of the convergence parameters with respect to this reference. The basis functions used are double-ζ for the s (DZS) and s,d (DZSD) orbitals. The lattice constant a and bulk modulus B were determined through a fitting to the Murnagham equation. All of the bulk modulus calculations were performed using an energy cutoff of 250 Ry.

				Au_2		Au_∞	
DFT	Basis	ΔE_{PAO} (mRy)	E_{cut} (Ry)	r_e (Å)	w_e (cm^{-1})	a (Å)	B (GPa)
LDA	DZS	10	60	2.463	205	4.054	207
	DZSD			2.468	208	4.084	201
		5		2.495	197	4.081	217
			100	2.460	202	4.069	207
GGA	DZS	10	60	2.537	172	4.181	152
	DZSD			2.541	165	4.202	139
		5		2.559	163	4.209	146
			100	2.525	186	4.160	152
LDA [a]	Plane Waves					4.07	190
GGA [a]	Plane Waves					4.19	132
Exp. [b]				2.47	191	4.06	172

[a]Reference 47.
[b]References 48 and 49.

we will show that our results are a very general consequence of metallic bonding. It is, therefore, important to have a simple and intuitive description of such bonding. From a structural point of view, some hallmarks of metals are: large plasticity; low temperature and enthalpy of melting, relative to cohesive energy; large ratio between bulk and shear moduli (Cauchy discrepancy); small vacancy formation energies relative to cohesion; contraction of surface interatomic distances, frequently leading to surface reconstructions. All these properties can be predicted by a class of ''metallic potentials,''[10,20,33–37] developed under different names (effective medium, embedded atom, glue model) and motivations (volume or coordination-dependent energy, second moment of the density of states, atomic inmersion in an electron gas) but which, ultimately, have a common functional form

$$E_{tot}=\sum_{i=1}^{N} E_i \tag{1}$$

$$E_i=\frac{1}{2}\sum_{j\neq i}\phi(r_{ij})+F(\overline{\rho}_i) \tag{2}$$

$$\overline{\rho}_i=\sum_{j\neq i}\rho(r_{ij}), \tag{3}$$

where $\phi(r_{ij})$ is mostly a repulsive pair potential, and the ''glue'' term $F(\overline{\rho}_i)$ can be rationalized as the inmersion energy of atom i in an electron gas of density $\overline{\rho}_i$, created by its neighbors' electron charge $\rho(r_{ij})$ [Eq. (3)]. The key ''metallic-bond'' ingredient lies in the nonlinearity of $F(\overline{\rho})$. According to effective medium theory, it first decreases (except for closed-shell atoms) as the empty valence levels are filled, and then increases again as a consequence of electron repulsion. In an alternative rationalization, in terms of the second moment of the density of states, it is a purely attractive term. However, one can always add and subtract a linear

TABLE II. Convergence tests of the energy difference between the most stable amorphous E_{am} and ordered E_{ord} cluster structures, for increasingly accurate approximations of the first principles calculations. The ordered structures are the Au_{38} truncated octahedron, the Au_{55} Mackay icosahedron, and the Au_{75} Marks decahedron. The amorphous structures are the lowest energy ones obtained with the Gupta potential. All structures were relaxed with the first principles method. The basis functions used are double-ζ for the s (DZS) and s,d (DZSD) orbitals. We have checked that the inclusion of f polarization orbitals changes the relative energies by only $\sim$0.05 eV. See text for the meaning of ΔE_{PAO} and E_{cut}

				$E_{am}-E_{ord}$ (eV)		
DFT	Basis	ΔE_{PAO} (mRy)	E_{cut} (Ry)	Au_{38}	Au_{55}	Au_{75}
LDA	DZS	10	60	−0.505	−0.143	−0.004
GGA	DZS	10	60	−0.114	−0.001	+0.304
GGA	DZS	5	100	−0.713	−0.229	−0.069
GGA	DZSD	5	100	−0.608	−0.357	−0.214

TABLE III. Energy difference $E_{am}-E_{ord}$ (in eV) between the most stable amorphous and ordered structures, using different metallic potentials. The structures are the same as in the previous table, and were relaxed with each potential.

Potential	Au_{38}	Au_{55}	Au_{75}
Gupta (Ref. 20)	−0.014	−0.515	+0.419
Embedded atom (Ref. 33)	−0.745	−1.132	−0.128
Sutton-Chen (Ref. 36)	+0.115	−0.409	+0.548
Glue model (Ref. 10)	−1.800	-6.170	+1.328

term to $F(\overline{\rho})$ and $\phi(r)$, so that $F(\overline{\rho})$ has a minimum at the ''optimum'' value of $\overline{\rho}$, i.e., that achieved at the most stable crystal phase.[10]

For our purposes, the most important consequence of the glue term, compared to purely pairwise potentials, is that an atom can largely compensate a coordination deficit by reducing its interatomic distances, in order to recover its ''optimal'' $\overline{\rho}$. And such a compensation also occurs for distance disorder, i.e., large and small interatomic distances compensate each other. This simple concept suffices to explain all the hallmarks of metallic bonding previously mentioned and, as we will see, it is also the key to understand the stability of amorphous metallic clusters.

Even with a common functional form, different methods using very different parametrization schemes result in different quantitative predictions. Attempts to describe bulk properties as accurately as possible may lead to overparametrization and to a poor transferability at the low coordination of the small clusters. Therefore, for global structure minimizations, we have used the Gupta potential,[20,38] which has only two independent parameters (apart from the length and energy scales) to fit two of the three basic functions $[\phi(r),F(\overline{\rho})$, and $\rho(r)]$ of Eqs. (2)–(3), with $F(\overline{\rho})=\sqrt{\overline{\rho}}$ fixed by the second moment of the density of states approximation. And, unlike the Sutton-Chen potential[36] used by Doye and Wales[12] (which also has just two parameters), the asymptotic behavior of $\phi(r)$ and $\rho(r)$ is described by a natural exponential form[39]

$$E_i=A\sum_{j\neq i} e^{-p(r_{ij}/r_b-1)}-\xi\left[\sum_{j\neq i} e^{-2q(r_{ij}/r_b-1)}\right]^{1/2}, \quad (4)$$

where r_b is the bulk-nearest neighbor distance, and the parameters A,ξ,p, and q are adjusted to make the crystal stable at that distance and to fit the cohesive energy and elastic constants.[38] Using this semiempirical potential, we have performed $\sim 10^5$ structure minimizations for each cluster size,[16,17] each one beginning from a different random geometry, using a genetic-symbiotic algorithm described elsewhere,[19] and relaxing the final structures.

In order to address the sensitivity of our results to the potential parametrization, we present in Table III the relative energy of the most stable amorphous and ordered structures, obtained with the Gupta potential, but relaxed again with different ''metallic'' potentials.[10,33,36] It can be seen that the amorphous structures of the smaller clusters are more stable in all cases, except with the Sutton-Chen potential. However, even with this potential the energy differences are very small and the general trends also hold.[17]

IV. ORIGIN OF AMORPHOUS STRUCTURES

The characterization of the local minima found for the three cluster sizes studied has been presented elsewhere.[17] Here, we only make a summary of their main features. For Au_{38}, the global minimum (always with the Gupta potential) is a disordered structure based on distorted decahedra on top of each other and capped with additional atoms. It is followed in energy by the truncated octahedron, by another disordered geometry only 15 meV above it, and by a near continuum of amorphous structures beginning ~ 0.1 eV above the global minimum. For Au_{55}, there are about 360 disordered geometries with energies below the Mackay icosahedron, which is the most stable ordered structure. For Au_{75}, the Marks' decahedron is the structure with lowest energy, but there are ~ 100 disordered geometries within an energy of 0.75 eV above it.[17]

As explained in Refs. 16,18, and confirmed in the more refined DFT calculations presented above, the relative energy ordering between the most stable ordered and amorphous structures obtained with the majority of the potential models is confirmed. In fact, our most accurate calculations bring the amorphous structure below the ordered one even for Au_{75}, although by a smaller energy than for Au_{38} and Au_{55}.

As an important first step in identifying the physical origin of cluster amorphization, we need to characterize the most relevant features of the stable disordered structures. First of all, it should be mentioned that our use of the terms ''amorphous'' and ''disordered,'' applied to clusters, does not mean that these geometries are absent of any order. Like in bulk liquids and amorphous solids, there is a lot of short-range order in ''disordered'' clusters. Furthermore, we cannot simply rely in a formal definition of disorder as absence of point group symmetries, because even crystalline clusters have no such symmetry except for some special sizes. Therefore, we simply mean here that most of the clusters that we characterize as amorphous have many typical amorphouslike features, for example in their pair correlation functions. A systematic analysis of the disordered cluster structures can be performed using, for example, the common-neighbor method[40] to identify the short-range order. Preliminary results of this analysis for Au_{55} have been published already[11]. We leave a more complete characterization of all the local-minima structures for future works,[41] and we concentrate here on the structural properties most relevant to the physical mechanism behind the amorphization tendency.

Figure 1 shows the electron density, obtained through the DFT-LDA calculation, as a function of the distance from the center of mass (CM) of the clusters. Since the electron den-

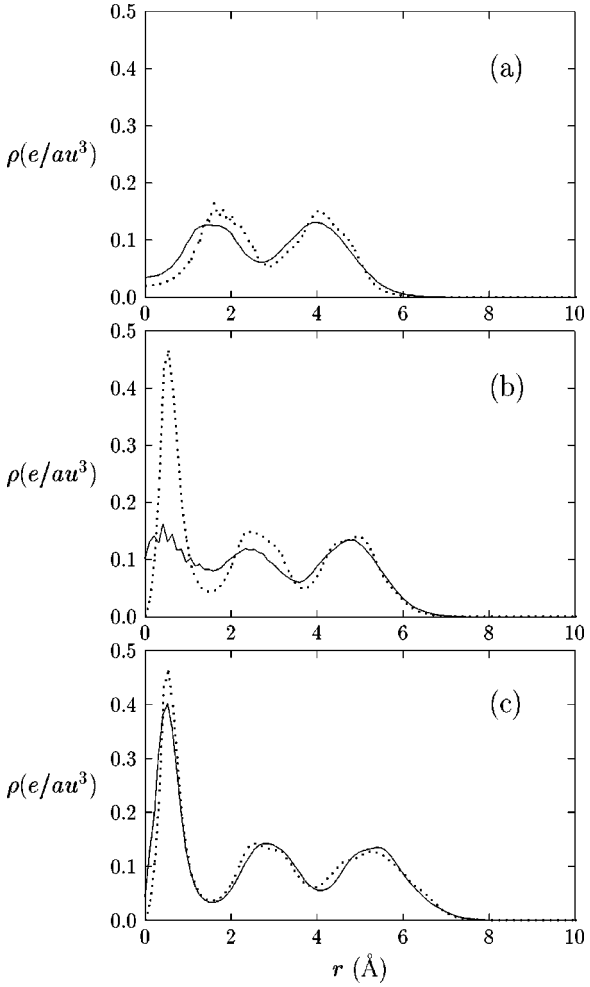

FIG. 1. Valence (pseudo) electron density as a function of distance from the center of mass (CM) for several clusters: (a) Au_{38}, (b) Au_{55}, (c) Au_{75}. Continuous lines: amorphous clusters; dotted lines: ordered clusters. The first peak in Au_{55} and Au_{75} originates from the d electron wavefunctions of the central atom, which behave as r^2 for $r \to 0$.

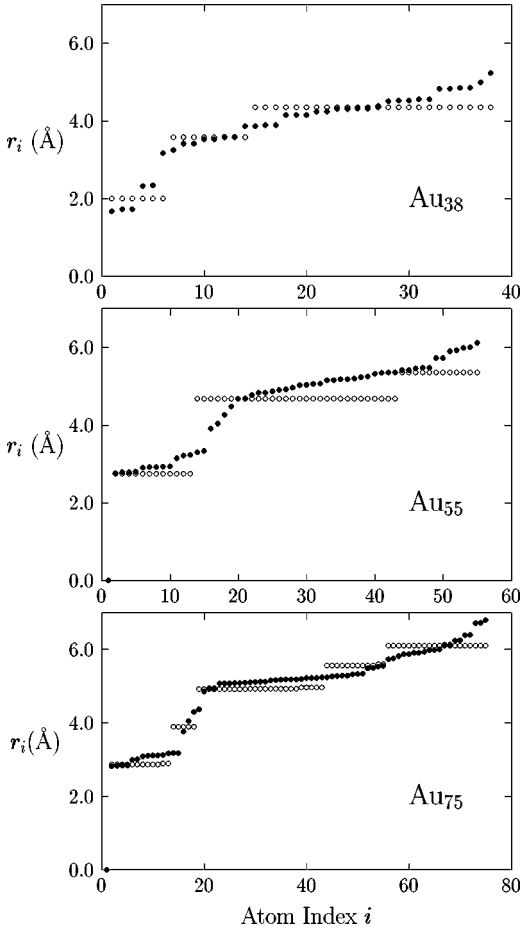

FIG. 2. Distances of the atoms from the center of the cluster, defined as the CM for Au_{38} and as the position of the central atom (closest to the CM) for Au_{55} and Au_{75}. Closed circles: amorphous clusters; open circles: ordered clusters.

sity is dominated by the d electrons, which are tightly bound to the atoms, the figure emphasizes the strong layering of atoms in spherical shells. The similarity of such a layering in the ordered and disordered structures is striking. In the case of Au_{38}, none of those structures has a central atom, and there are only two well-defined shells. In Au_{55} and Au_{75}, there is an atom in the center but there are still only two well-defined shells. This is not surprising for Au_{55}, whose icosahedral structure closes the second atomic shell, but it is striking for Au_{75}, which has 20 additional atoms.

Figure 2 shows the distance of the atoms from the CM. The atomic shells are not so clear, but they can still be identified between radial regions of low-atom concentration. In comparing the ordered and disordered structures, one notices ''atomic transfers'' among shells. In Au_{38}, the octahedron of the inner shell loses one atom and becomes a trigonal bipyramid. In Au_{55} and Au_{75}, the central 13-atom icosahedron gains two atoms, forming in both cases the same peculiar structure, with 14 atoms around a central one.

Why should the compact, high-symmetry central structures change to something much less symmetric and compact? This is surprising because one might expect that most of the changes occur at the surface, where the atoms will try to increase their coordination (explaining the extensive reconstructions that occur in the bulk surfaces). In fact, total coordination count cannot explain the stability of the amorphous clusters: although it increases in Au_{38} and Au_{75}, it considerably decreases for Au_{55} despite which the energy gain (the energy difference between the amorphous and ordered structures) is the largest of the three cluster sizes.

To answer this question, we have plotted in Fig. 3 the atomic energies E_i, defined in Eq. (2). It can be seen that most of the energy gain occurs indeed in the central region of the cluster. Since the coordination there is nearly perfect, this fact clearly points to an elastic energy contribution. In fact, elastic energy is a determinant contribution to cluster structure also with pair potentials: as the cluster size increases, the compact icosahedral structures accumulate too much elastic energy and change first to decahedral and later to fcc structures.[23] This tendency increases with decreasing range of the potential, because this correlates with a narrower potential well, and with larger elastic constants. Thus, with pair potentials, amorphous structures have a larger elastic energy and appear preferentially for longer interaction ranges. As mentioned previously, we observe the opposite tendency: the amophous structures are stable for gold clusters, but not for other metals with a longer potential range.[17] So, something else must be playing a role.

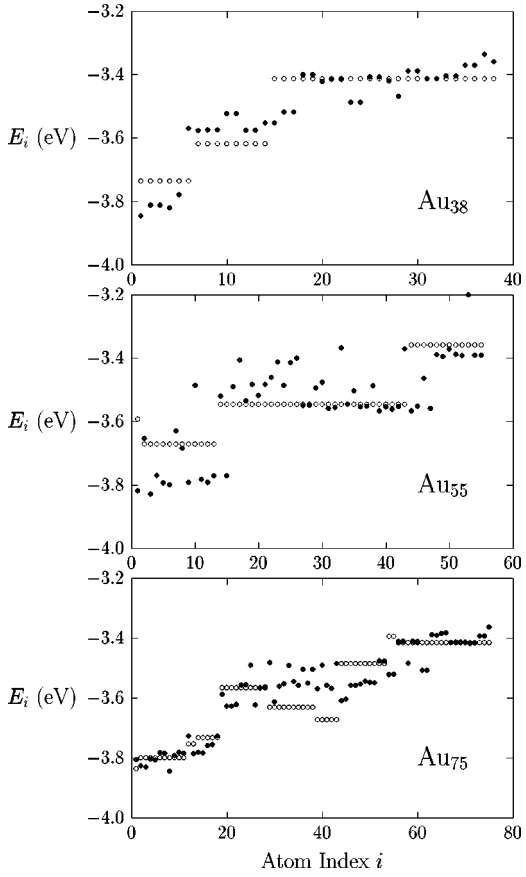

FIG. 3. Energies E_i of the atoms, ordered by their distance from the CM. See text for the definition of E_i. Symbols as in Fig. 2.

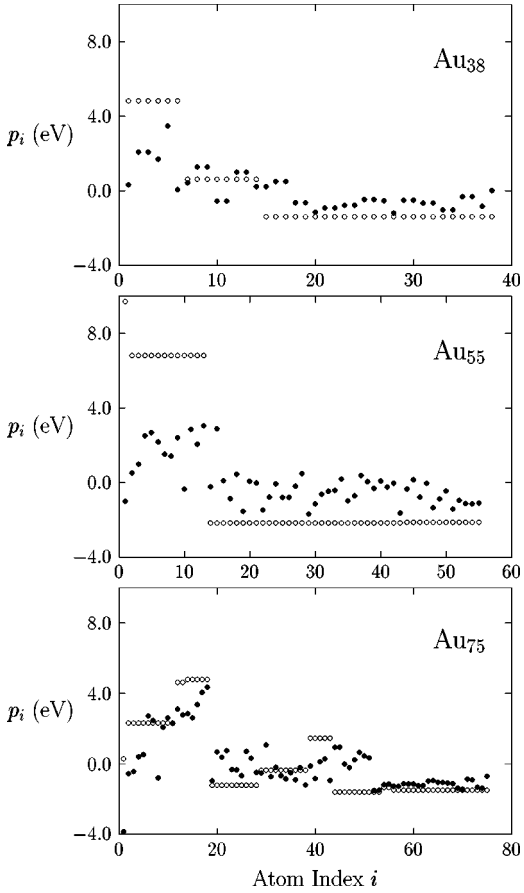

FIG. 4. Local atomic pressures p_i, with atoms ordered by their distance from the CM. See text for the definition of atomic pressure. Symbols as in Fig. 2.

In order to study elastic effects, Doye and Wales[23] split the cluster's total energy into three components: nearest neighbors, elastic, and non-nearest neighbors. The first of these components is the sum of atomic energies including only the nearest-neighbors but at the optimum distance (for each atom). The second component is the energy increase for placing the nearest neighbors at their actual distance. Although very natural, in the case of amorphous structures this definition has the disadvantage of depending strongly on the cutoff radius for nearest neighbors. In order to avoid this ambiguity, we study the ''local,'' or ''atomic'' stress tensor, defined simply as

$$\sigma_i^{\mu\nu}=\frac{1}{\Omega}\frac{\partial E_i}{\partial \epsilon_{\mu\nu}}, \tag{5}$$

where, $\epsilon_{\mu\nu}$ is the strain tensor, and Ω is a constant volume (equal to the bulk atomic volume) used to recover the correct stress units. This local stress definition is parallel to the one recently proposed in real space.[42] Since the cluster is free to deform, in a local minimum the total stress satisfies $\Sigma_i \sigma_i^{\mu\nu}=0$. In Fig. 4, we plot the ''local'' pressure, obtained from the trace of the stress tensor: $p_i=-(1/3)\Sigma_\mu \sigma_i^{\mu\mu}$. We see that (i) the pressure is positive in the interior of the cluster, which is compressed by the surface, and (ii) the pressure is considerably reduced in the amorphous structures, relative to the ordered ones. This confirms the hypothesis that the ordered structures are de-stabilized by their high-elastic energy, which the less-constrained amorphous structures are able to reduce.

One may be tempted to assign point (i) to the liquidlike pressure induced by the surface tension of a curved surface. However, some care must be taken in making such an assignment. In a liquid, the tension occurs because the system tries to reduce the number of atoms on the surface. The lower atomic concentration means that the surface atoms are too far away, i.e., in the attractive region of the interatomic potential, and this produces the average tendency of the surface to contract. In a solid with a fixed structure, the surface *stress* may be positive or negative, large or small, without any given relationship with the surface *tension* (energy).[43] Therefore, there is still a point in asking why, in the case of gold clusters, the ordered structures have a specially high-surface stress, which induces a high pressure and a high-elastic energy.

The key to answer this question lies in the special character of the metallic bond, as explained before. In order to compensate for the lower coordination, the bonds tend to get shorter than in the bulk. Thus, the original bonds of the ordered structures, which were very stable with purely pairwise potentials, are now too long and have a high tendency to contract. We may expect this tendency to depend on how the optimum interatomic distance r [at which Eq. (2) is minimum], changes with the number of nearest neighbors n: $dr/dn=0$ for a pair potential, while $dr/dn>0$ for a metallic potential.

TABLE IV. Magnitudes that determine the tendency towards amorphization of metallic clusters, calculated from the potential parameters p and q of Ref. 37 and Eqs. (6)–(8). E is the energy per atom as a function of coordination n. $\overline{\delta E}$ is the mean energy increment produced by a dispersion $\overline{\delta r^2}$ in the interatomic distance r. We use $n=12$ for the bulk coordination. Au_{pp} denotes a Morse pair potential fitted to gold.

Element	Ni	Cu	Rh	Pd	Ag	Ir	Pt	Au	Au_{pp}
p	10.00	10.08	14.92	10.84	10.12	14.53	10.80	10.15	
q	2.70	2.56	2.51	3.67	3.37	2.90	3.50	4.13	
$(dr/dn)/r\times10^3$	5.71	5.54	3.36	5.81	6.17	3.58	5.71	6.92	0.00
$(dE/dn)/E\times10^2$	2.63	2.75	3.32	2.03	2.09	3.13	2.17	1.31	8.33
$(\overline{\delta E}/\overline{\delta r^2})/(E/r^2)$	8.92	8.88	15.3	10.6	9.25	16.3	10.6	7.78	20.25

The elastic energy of the ordered structure is the driving force for the cluster amorphization but, in order for it to occur, the energy increase due to the disorder must be small enough. This energy is associated to coordination defects and to bond-length dispersion. Thus, we may identify two variables opposing the amorphization, namely (a) the energy change for varying coordination dE/dn, and (b) the average energy change $\overline{\delta E}$ for a dispersion $\overline{\delta r^2}$ of the interatomic distances.

For a first qualitative analysis we will use an extremely simplified model: we ignore non-nearest-neighbor interactions and we assume that all the nearest neighbors are at the same distance r (except for the effect of distance disorder, see below). Although these would be very crude approximations to calculate absolute energies, they are adequate to identify the main factors leading to amorphous structures, and to extract simple trends across the periodic table. Then, Eq. (2) becomes $E(n,r)=(n/2)\phi(r)+F[n\rho(r)]$ and, for the model of Eq. (4) we obtain

$$\frac{dr}{dn}=-\frac{\partial^2E/\partial n\partial r}{\partial^2E/\partial r^2}=\frac{r/n}{2(p-q)} \tag{6}$$

$$\frac{dE}{dn}=\frac{\partial E}{\partial n}=\frac{p-2q}{2(p-q)}\frac{E}{n} \tag{7}$$

$$\frac{\overline{\delta E}}{\overline{\delta r^2}}=\frac{n}{2}\left[\frac{1}{2}\phi''(r)+F'(\overline{\rho})\rho''(r)+F''(\overline{\rho})\rho'(r)^2\right]$$

$$=-\frac{pq(p-2q+q/n)}{2(p-q)}\frac{E}{r^2}, \tag{8}$$

where we take the derivatives at the bulk parameters n,r, at which $\partial E/\partial r=0$. In Table IV, we present these magnitudes for several metals, using the parameters of Ref. 38, as well as a Morse pair potential fitted to reproduce the lattice constant, cohesive energy, and bulk modulus of gold. Two important points can be noticed: (i) compared to a pairwise interaction (and besides the nonzero bond contraction dr/dn), the metallic bonding pays a very low price for the disorder in coordination and bond lengths induced by amorphization (low values of dE/dn and of $\overline{\delta E}/\overline{\delta r^2}$); (ii) among all the metals in the table, gold has the highest value of dr/dn (i.e., the largest contraction of surfaces bonds), and the lowest values of dE/dn and $\overline{\delta E}/\overline{\delta r^2}$ (i.e., the smallest cost of amorphization).

V. TRENDS OF CLUSTER AMORPHIZATION

In order to obtain the tendencies of Table IV directly from experimental magnitudes, and to extend it to other metals, we will express the cluster's energy, within our simplified model, as

$$E_{tot}(r)=N_sE(n_s,r)+N_bE(n_b,r)$$

$$\simeq N_s(n_s-n_b)\frac{\partial E}{\partial n}+(N_s+N_b)E(n_b,r), \tag{9}$$

where (N_s,N_b) are the numbers of surface and interior (bulk) atoms, and (n_s,n_b) are the corresponding numbers of nearest neighbors of those atoms. We are assuming here that all the bonds of the ordered cluster have the same length r. Expanding $E(n,r+\delta r)$ around (n_b,r), to second order, the distortion energy is

$$\delta E_{tot}=N_s(n_s-n_b)\frac{\partial^2E}{\partial n\partial r}\delta r+\frac{N}{2}\frac{\partial^2E}{\partial r^2}\delta r^2, \tag{10}$$

where $N=N_s+N_b$. The first term is the decrease in surface energy and the second one is the elastic energy δE_{el}. Minimizing with respect to δr, we find that the resulting elastic energy per atom is

$$\delta E_{el}=\frac{N_s^2(n_b-n_s)^2}{2N}\frac{(\partial^2E/\partial n\partial r)^2}{\partial^2E/\partial r^2}. \tag{11}$$

For cubic and hexagonal close packing, the partial derivatives in Eqs. (10) and (11) are related[44] to the Voigt-averaged bulk and shear moduli B and G

$$\frac{\partial^2E}{\partial r^2}=\frac{9\Omega}{r^2}B \tag{12}$$

$$\frac{\partial^2E}{\partial n\partial r}=\frac{3\Omega}{nr^2}\frac{\rho(r)}{\rho'(r)}(3B-5G). \tag{13}$$

The parenthesis in Eq. (13) is proportional to the ''Cauchy pressure,''[34] which cancels with purely pairwise potentials. Ω is the bulk atomic volume. $\rho(r)/\rho'(r)=\{d\log[\rho(r)]/dr\}^{-1}$ is the decay length of the atomic electron density, roughly proportional to the equilibrium interatomic distance r. For the Gupta potential [Eq. (4)], $\rho(r)/\rho'(r)=r/2q$ and, using an average value of q, we approximate $\rho(r)/\rho'(r)\simeq r/6.3$. As an estimate of the amor-

TABLE V. Ratio between the elastic energy of the ordered clusters, and their amorphization energy, calculated from Eq. (14). Experimental data for the bulk (B) and shear (G) modulii were taken from Ref. 50 (values with asterisks from Ref. 51). The atomic volume and enthalpy of melting were obtained from Ref. 51. To our knowledge, elastic constants for bulk B and Tc are not available. For elements with a negative Cauchy pressure $(3B-5G)/2$ we set the elastic energy to zero.

Li	**Be**						**Element**					**B**		
13.00	4.88						Ω (cm^3/mol)					4.62		
12.0	111.7						B (GPa)							
6.2	151.8						G (GPa)							
4.60	9.80						ΔH_{melt} (kJ/mol)					22.2		
0.09	0						$\delta E_{el}/N$ (kJ/mol)							
0.02	0						$\delta E_{el}/\delta E_{am}$							
Na	**Mg**											**Al**	**Si**	
23.68	13.98											10	12.06	
6.8	35.2											77.3	97.7	
2.8	17.4											26.2	67.7	
2.64	9.04											10.67	39.60	
0.41	0.44											4.13	0	
0.15	0.05											0.39	0	
K	**Ca**	**Sc**	**Ti**	**V**	**Cr**	**Mn**	**Fe**	**Co**	**Ni**	**Cu**	**Zn**	**Ga**	**Ge**	
45.36	25.86	15.04	10.55	8.34	7.23	7.38	7.09	6.62	6.59	7.09	9.17	11.81	13.64	
3.3	10.7	55.8	105.0	156.7	159.3	59.6*	166.7	193.3	184.3	137.7	72.7	58.6	75.0	
1.2	8.8	30.9	44.2	47.9	116.0	79.5*	89.2	86.0	92.0	54.6	46.6	38.4	56.5	
2.40	9.33	15.90	20.90	17.60	15.30	14.40	14.90	15.20	17.60	13.00	6.67	5.59	34.70	
0.62	0	0.15	2.77	8.83	0	0	0.39	2.41	0.97	3.16	0	0	0	
0.28	0	0.01	0.13	0.50	0	0	0.03	0.16	0.05	0.24	0	0	0	
Rb	**Sr**	**Y**	**Zr**	**Nb**	**Mo**	**Tc**	**Ru**	**Rh**	**Pd**	**Ag**	**Cd**	**In**	**Sn**	**Sb**
55.79	34.50	19.89	14.02	10.84	9.39	8.6	8.14	8.29	8.85	10.27	13.00	15.71	16.24	18.20
2.6	11.5	41.2	96.7	169.7	265.0		310.9	267.0	190.0	102.0	59.0	42.2	57.0	43.3
1.1	4.4	25.5	36.8	39.6	124.8		191.6	154.2	53.2	33.3	25.8	5.9	20.1	33.8
2.20	9.16	17.20	23.00	27.20	27.60	23.81	37.70	21.55	17.20	11.30	6.11	3.27	7.20	20.90
0.42	1.46	0	5.11	19.3	3.24		0	0.09	13.5	6.12	1.57	11.02	4.41	0
0.19	0.16	0	0.22	0.71	0.12		0	0.004	0.78	0.54	0.26	3.37	0.61	0
Cs	**Ba**	**Lu**	**Hf**	**Ta**	**W**	**Re**	**Os**	**Ir**	**Pt**	**Au**	**Hg**	**Tl**	**Pb**	**Bi**
70.96	38.21	17.78	13.41	10.87	9.53	8.86	8.43	8.57	9.10	10.19	14.81	17.24	18.26	21.44
1.8	10.3*	47.7	108.8	191.3	307.7	365.0	373.0*	373.3	283.0	170.7	22.4	35.7	43.9	26.4
1.4	4.9*	27.6	56.0	70.8	157.0	180.7	223.0*	230.0	65.1	31.2	16.5	6.2	10.4	17.5
2.09	7.66	19.20	25.50	31.40	35.20	33.10	29.30	26.40	19.70	12.70	2.33	4.31	5.12	10.48
0	0.50	0.03	0.80	8.61	1.84	2.78	0.001	0	27.54	23.66	0	8.76	8.28	0
0	0.07	0.002	0.03	0.27	0.05	0.08	0.000	0	1.40	1.86	0	2.03	1.62	0

phization energy, we simply use the enthalpy of melting $\delta E_{am}=N\Delta H_{melt}$, and we take $n_s \simeq n_b/2$ to obtain

$$\frac{\delta E_{el}}{\delta E_{am}} \simeq \frac{\Omega(3B-5G)^2}{320B\Delta H_{melt}}\left(\frac{N_s}{N}\right)^2. \tag{14}$$

This equation correctly predicts a decreasing amorphization tendency for increasing cluster size but, for $N \leqslant 100$, the majority of the atoms are on the surface, and we can take $N_s/N \sim 1$. The result of this analysis is presented in Table V. It can be seen that the amorphization tendency increases from left to right and downwards in the periodic table, pointing to gold with the highest tendency (except column 3A). It is also interesting to notice that the two transition metals with highest tendency to amorphization are Pt and Pd, since the possible existence of amorphous clusters of these metals might have enormous implications for catalysis. Work is in progress to study this possibility. Yang *et al.*[24] already found that the most stable calculated structures of Pt_{13}, also a magic size, were amorphouslike.

The results of Table V for the elements of column 3A are especially remarkable. However, it should be noted tha Ga, In, and Tl have complex structures, while Eq. (13) is exact only for cubic and hcp structures. Also, it must be emphasized that the above oversimplified model assumes that the Cauchy discrepancy is entirely due to metallic binding. In a more complete treatment, other effects, like directional covalent bonding, might also play an important role. In fact, in several cases we find a negative Cauchy pressure $(3B-5G)/2$, incompatible with the assumed purely metallic interaction, and we have arbitrarily set to zero the elastic energy in those cases.

One may wonder why, if metals have such a strong tendency towards amorphization, it is so difficult to produce pure amorphous metals. The causes are purely kinetic: the

same reasons that lower the energy of liquid and amorphous metals, also lower the energy barriers between different structures. This means that the system can easily find the lowest energy structure (i.e., the crystal in the case of bulk) and that tremendously high cooling rates are required to quench the liquid into an amorphous solid.[45,46]

VI. SUMMARY AND CONCLUSIONS

In summary, we have shown that an analysis of the local stress in gold nanoclusters provides a physical interpretation of the relative stability of amorphouslike structures with respect to ordered configurations. We found that the key factors that favor the amorphization of gold nanoclusters are the tendency of metallic bonds to contract at the cluster surface due to a reduced coordination and also the low-energy cost associated to bond length and coordination disorder in metals. These are characteristic properties of the metallic bonding which are enhanced in the case of gold. A general trend for the possible amorphization of other metal clusters was presented. It shows an increment in the amorphization tendency for metals from left to right and downwards in the periodic table.

The analysis of the cluster structures and energetics presented in this work corresponds to isolated bare-gold nanoclusters. The structural characterization, through XRPD,[8,9] of these systems has been performed using samples passivated with thiol molecules. Although we have found a better agreement between the calculated and experimental structure factors using the bare amorphouslike structures compared to the ordered configurations,[17] it is probable that the thiol-metal interaction will modify the amorphization trend presented in this paper. In particular, one of the key factors which favor the amorphization, the reduced coordination at the cluster surface, will decrease due to the presence of thiol molecules. In that case, the thiols will not only play a role as passivating agents but also stabilizing the cluster structure. This picture is in contrast with that presented in Refs. 8 and 14, according to which the gold nanoclusters are originally in ordered configurations, without any major structural change produced by the thiol interactions. We consider, however, that any realistic study of the effect that thiol molecules produce on gold nanocluster properties should contemplate the amorphous cluster structures. Work is currently in progress to elucidate this effect.

ACKNOWLEDGMENTS

This work was supported by Spain's DGES Grant No. PB-0202, Mexico's CONACYT Grant No. 25083-E, DGAPA-UNAM Grant No. IN101297, and DGSCA-UNAM Supercomputing Center. J.M.S. and I.L.G. thank Spain's SEUID for financial support. D.S.P. acknowledges support from Grants Nos. DOE 8371494 and DEFG 02/96/ER 45439.

[1] R.L. Whetten, J.T. Khoury, M.M. Alvarez, S. Murthy, I. Vezmar, Z.L. Wang, P.W. Stephens, C.L. Cleveland, W.D. Luedtke, and U. Landman, Adv. Mater. **5**, 8 (1996).

[2] R.P. Andres, T. Bein, M. Dorogi, S. Feng, J.I. Henderson, C.P. Kubiak, W. Mahoney, R.G. Osifchin, and R. Reifenberger, Science **272**, 1323 (1996).

[3] C.A. Mirkin, R.L. Letsinger, R.C. Mucic, and J.J. Storhoff, Nature (London) **382**, 607 (1996).

[4] A.P. Alivisatos, K.P. Johnsson, X. Peng, T.E. Wilson, C.J. Loweth, M.P. Bruchez, Jr., and P.G. Schultz, Nature (London) **382**, 609 (1996).

[5] R.P. Andres, J.D. Bielefeld, J.I. Henderson, D.B. Janes, V.R. Kolagunta, C.P. Kubiak, W.J. Mahoney, and R.G. Osifchin, Science **273**, 1690 (1996).

[6] W.D. Luedtke and U. Landman, J. Phys. Chem. **100**, 13 323 (1996).

[7] C.L. Cleveland, U. Landman, M.N. Shafigullin, P.W. Stephens, and R.L. Whetten, Z. Phys. D: At., Mol. Clusters **40**, 503 (1997).

[8] C.L. Cleveland, U. Landman, T.G. Schaaff, M.N. Shafigullin, P.W. Stephens, and R.L. Whetten, Phys. Rev. Lett. **79**, 1873 (1997).

[9] T.G. Schaaff, M.N. Shafigullin, J.T. Khoury, I. Vezmar, R.L. Whetten, W.G. Cullen, P.N. First, C. Gutiérrez-Wing, J. Ascensio, and M.J. Yacamán, J. Phys. Chem. **101**, 7885 (1997).

[10] F. Ercolessi, W. Andreoni, and E. Tosatti, Phys. Rev. Lett. **66**, 911 (1991).

[11] I.L. Garzón and A. Posada-Amarillas, Phys. Rev. B **54**, 11 796 (1996).

[12] J.P.K. Doye and D.J. Wales, New J. Chem. **22**, 733 (1998).

[13] O.D. Häberlen, S.C. Chung, M. Stener, and N. Rösch, J. Chem. Phys. **106**, 5189 (1997).

[14] H. Häkkinen, R.N. Barnett, and U. Landman, Phys. Rev. Lett. **82**, 3264 (1999).

[15] J.A. Ascencio, C. Gutiérrez-Wing, M.E. Espinosa, M. Marín, S. Tehuacanero, C. Zorrilla, and M.J. Yacamán, Surf. Sci. **396**, 349 (1998).

[16] I.L. Garzón, K. Michaelian, M.R. Beltrán, A. Posada-Amarillas, P. Ordejón, E. Artacho, D. Sánchez-Portal, and J.M. Soler, Phys. Rev. Lett. **81**, 1600 (1998).

[17] K. Michaelian, N. Rendón, and I.L. Garzón, Phys. Rev. B **60**, 2000 (1999).

[18] I.L. Garzón, K. Michaelian, M.R. Beltrán, A. Posada-Amarillas, P. Ordejón, E. Artacho, D. Sánchez-Portal, and J.M. Soler, Eur. J. Phys. D (to be published).

[19] K. Michaelian, Am. J. Phys. **66**, 231 (1998); Chem. Phys. Lett. **293**, 202 (1998).

[20] R.P. Gupta, Phys. Rev. B **23**, 6265 (1981).

[21] D.J. Wales, Science **271**, 925 (1996).

[22] T.P. Martin, Phys. Rep. **273**, 199 (1996).

[23] J.P.K. Doye and D.J. Wales, J. Phys. B **29**, 4859 (1996).

[24] S.H. Yang, D.A. Drabold, J.A. Adams, P. Ordejon, and K. Glassford, J. Phys.: Condens. Matter **9**, L39 (1997).

[25] P. Ordejón, E. Artacho, and J.M. Soler, Phys. Rev. B **53**, 10 441 (1996); D. Sánchez-Portal, P. Ordejón, E. Artacho, and J.M. Soler, Int. J. Quantum Chem. **65**, 453 (1997).

[26] E. Artacho, D. Sánchez-Portal, P. Ordejón, A. García, and J.M. Soler, Phys. Status Solidi B **215**, 809 (1999).

[27] W. Kohn and L.J. Sham, Phys. Rev. **145**, 561 (1965).
[28] N. Troullier and J.L. Martins, Phys. Rev. B **43**, 1993 (1991).
[29] L. Kleinman and D.M. Bylander, Phys. Rev. Lett. **48**, 1425 (1982).
[30] O.F. Sankey and D.J. Niklewski, Phys. Rev. B **40**, 3979 (1989).
[31] W.H. Press, S.A. Teukolsky, W.T. Vetterling, and B.P. Flannery, *Numerical Recipes. The Art of Scientific Computing* (Cambridge University Press, Cambridge, 1992).
[32] W.A. de Heer, Rev. Mod. Phys. **65**, 611 (1993).
[33] M.S. Daw and M.I. Baskes, Phys. Rev. B **29**, 6443 (1984).
[34] M.W. Finnis and J.E. Sinclair, Philos. Mag. A **50**, 45 (1984).
[35] K.W. Jacobsen, J.K. Nørskov, and M.J. Puska, Phys. Rev. B **35**, 7423 (1987).
[36] A.P. Sutton and J. Chen, Philos. Mag. Lett. **61**, 139 (1990).
[37] S.M. Foiles, Mater. Res. Bull. **21**, 24 (1996).
[38] V. Rossato, M. Guillope, and B. Legrand, Philos. Mag. A **59**, 321 (1989).
[39] I.J. Robertson, V. Heine, and M.C. Payne, Phys. Rev. Lett. **70**, 1944 (1993).
[40] D. Faken and H. Jónsson, Comput. Mater. Sci. **2**, 279 (1994), and references therein.
[41] The atomic coordinates are available upon request from the authors.
[42] A. Filippetti and V. Fiorentini, cond-mat/9907360 (unpublished).
[43] However, for the same reasons as in the liquid, solid structures with a lower surface concentration of atoms, and with longer surface interatomic distances, may be expected to have a lower energy. This is what stabilizes the icosahedral structures with pair potentials. Therefore, an *ensemble* of solid clusters will show on average a contractive surface stress, and a positive pressure inside, like in the liquid.
[44] D.J. Oh and R.A. Johnson, J. Mater. Res. **3**, 471 (1988).
[45] A. Posada-Amarillas and I.L. Garzón, Phys. Rev. B **53**, 8363 (1996).
[46] O. Rodriguez de la Fuente and J.M. Soler, Phys. Rev. Lett. **81**, 3159 (1998).
[47] B.D. Yu and M. Scheffler, Phys. Rev. B **46**, R15 569 (1997).
[48] K.P. Huber and G. Herzberg, *Molecular Spectra and Molecular Structure Constants of Diatomic Molecules* (Van Nostrand, New York, 1979).
[49] C. Kittel, *Introduction to Solid State Physics* (Wiley, New York, 1996).
[50] *Numerical Data and Functional Relationships in Science and Technology*, edited by K.-H. Hellwege, Landolt-Börnstein, New Series, Group III, Vol. 11 (Springer-Verlag, Berlin, 1979).
[51] J. Emsley, *The Elements* (Clarendon Press, Oxford, 1998).